Entropy considerations also would be expected to favor E over B.[19] The freezing out of an internal rotational mode of HOH by forming a bifurcated structure rather than a linear one plus the double degeneracy of the linear H-bonded structure would be expected to stabilize the E structure by ~1 kcal/mol at 298 K, thus reducing the preference for the B relative to the E″ structure of $HCOO^-\cdots H_2O$ and $(CH_3O)_2PO_2^-\cdots H_2O$.

However, such a bifurcated structure may be kinetically important in general base catalysis by $HCOO^-$. For example, in the 6-31G** calculations, Mulliken populations suggest that the B structure H_2O has a slightly more negative charge (−0.071) than the E″ (−0.067) as well as a somewhat more negative oxygen (−0.783 (B) and −0.771 (E″)). Thus, the B H_2O may be slightly more effective than E in its nucleophilic attacks on electrophiles.

Finally, it is worth relating our calculations to the analysis of bifurcated carbohydrate H bonds by Jeffrey and Maluszynska.[20] These authors have found many examples of

bifurcated H bonds in these crystals, attributing this to the greater density of –O– acceptors than hydroxyl hydrogens. Ab initio calculations by Newton et al.[21] support the notion that such "nonoptimal" bifurcated hydrogen bonds can be more stable than a single linear H bond (see Table II in ref 21), analogously to what has been found in this study.

There are three important points to emerge from this study.

First, it represents the most definitive demonstration of how the lowest energy structure determined from single solvation site calculations (B structure) is very little represented[4,5] when one considers multiple solvation. This underscores the danger of extrapolating single water hydration studies to infer properties of the aqueous solution structure and the importance of Monte Carlo or Molecular Dynamics simulations of each solutions. In such a Monte Carlo study[5] of the aqueous solvation of $(CH_3O)_2PO_2^-$, we have shown that the water interactions with the PO_2^- are predominantly of the E type.

Secondly, this study supports the preferential use of molecular mechanical (empirical potential) methods over minimal basis set ab initio (STO-3G) or, by inference, semiempirical MO methods that are based on reproducing minimal basis set ab initio studies, for studying molecular interactions. We should emphasize, however, that minimal basis sets derived by SCF atom calculations (e.g., those used in ref 14) do not suffer the same defect as STO-3G.

Finally, the calculations suggest that, for cases in which a single water molecule interactions with molecules where there is more than one center of partial negative charge, e.g., BH_4^-, $RCOO^-$, RPO_2^-, the bifurcated structure will be the one of minimum energy. In the case of the bifurcated $RPO_2^-\cdots H_2O$ structure, each $O^{\delta-}\cdots H–O$ hydrogen bond is significantly ($\angle OOH = 26.2°$ for $R_{O\text{-}H} = 2.10$ Å) bent, but two bent bonds appear to be more stabilizing that one ideal linear one. Thus, in systems such as $–XO_2^-$, one could imagine a dependence of the relative stabilities of B and E on OXO angle and XO bond length. Those geometrical changes which would allow more linear $O–H\cdots O^{\delta-}$ interactions in the B structure would tend to stabilize this structure; those that make these interactions less linear would stabilize the E structures.

Note Added in Proof. We have been made aware of ab initio calculations on nitrate and nitrite anion hydration using a 6-31G basis set (J. M. Howell, A. M. Sapse, E. Singman, and G. Snyder, *J. Chem. Phys.*, **86**, 2345–2349 (1982)), which found more stable bifurcated than linear structures for NO_2^- and NO_3^-.

Acknowledgment. We gratefully acknowledge the support of the NIH (CA-25644 and GM-29072) to P.A.K. and helpful discussions with U. C. Singh on the use of Gaussian 80 UCSF. One of us (G.A.) has been partially supported by C.N.R. through a NATO Senior Fellowship.

Registry No. $(CH_3O)_2PO_2^-$, 7351-83-9; $HCOO^-$, 71-47-6; H_2O, 7732-18-5.

(19) Assuming the relative 4-31G energies of E and E″ in Table II, only the E″ would contribute to the thermodynamic properties and there would be one E″ structure for each oxygen. Thus, the degeneracy of 2 for E″. In addition, the internal rotation of the external water O–H in the E″ structure, but not the B, would lead to an additional contribution of 0.5 entropy unit (assuming a frequency of 300 cm^{-1}) for this structure. The sum of these two would be 2 e.u. or 0.6 kcal/mol at 300 K.

(20) G. Jeffrey and H. Maluszynska, *Int. J. Quant. Chem., Quant. Biol. Symp.*, **8**, 231 (1981).

(21) M. Newton, G. Jeffrey, and S. Takagi, *J. Am. Chem. Soc.*, **101**, 1997 (1979).

Luminescence Quenching Studies in NaLS Micellar Systems at 77 K

S. Hashimoto and J. K. Thomas*

Contribution from the Chemistry Department, University of Notre Dame, Notre Dame, Indiana 46556. *Received February 3, 1983*

Abstract: The formation of a micellar structure of sodium lauryl sulfate (NaLS) in an ethylene glycol–water mixture (EGW) both at room temperature and at 77 K was confirmed by using photochemical techniques. An aggregation number of 29 was determined in 0.050 M NaLS in 45% v/v ethylene glycol–water both at room temperature (20 °C) and at 77 K. Luminescence studies of the quenching reactions of the lowest excited state of tris(2,2′-bipyridine)ruthenium(II) ($Ru(bpy)_3^{2+}$) by Cu^{2+}, Cr^{3+}, and Fe(III) in NaLS–EGW micellar solutions at 77 K exhibited unusual kinetics, which are attributed to energy transfer or electron-transfer processes from the excited Ru(II) complex to metal ions, all of which are randomly distributed on the micellar surface. In contrast to behavior at 77 K, the quenching of $*Ru(bpy)_3^{2+}$ by Cu^{2+} in a NaLS–EGW system at room temperature was explicable by simple Stern–Volmer kinetics, as observed in a NaLS micellar solution. On the other hand, the quenching behavior of the singlet excited pyrene by 1-ethyl-1′-hexadecyl-4,4′-bypyridinium ($C_{16}C_2V^{2+}$) ion appeared to be quite similar, both at room temperature and at 77 K. This latter effect was explained by an electron-tunneling mechanism where electron transfer takes place between species which are separated by distances that are larger than that of the closest contact of the quenchee–quencher pair at room temperature. Consequently, the micellar system at 77 K offers a reaction medium, being unique in its rigidity which fixes reactants in a known geometry in space, a situation which does not occur in homogeneous systems at this temperature. This effect can also be ascribed to a "catalytic" feature of micelles.

There have been numerous studies over the past several years of photochemical reactions in organized assemblies such as micelles, microemulsions, vesicles, etc.[1] Micelles have attracted much attention by two inherent and important properties, first, their

0002-7863/83/1505-5230$01.50/0

ability to solubilize hydrophobic molecules, and second, that of binding ionic species to the micellar surface. The catalytic or inhibitory effect of micelles on the kinetics of a large variety of reactions, especially photoinduced electron-transfer reactions, has been reported.[1]

Electron-tunneling processes are also claimed to take place in micellar systems.[2] The complexity of the kinetics of a micellar system at room temperature[3] may depend upon the possibility of intramicellar diffusional motion of solutes, of the intermicellar solute exchange process through micelle–micelle collision, and of dynamic or open structures of the micelle itself.

Recently Kevan and co-workers[4] have shown the presence of micellar structures even in frozen solution. Inhibition of the diffusional motion by freezing may make it much easier to study reactions that take place in the absence of diffusional motion, such reactions as tunneling processes,[5] or actual static quenching. To overcome the difficulty of optical measurements in frozen micelles (i.e., ice) we attempted to make a micelle in frozen glassy solution.

In the present paper, positive evidence for micellar formation of sodium lauryl sulfate (NaLS) in an ethylene glycol–water mixture at room temperature and at 77 K is first described. The well-characterized emission-quenching reactions of singlet pyrene (Py*), and the excited state of tris(2,2′-bipyridine)ruthenium(II) (*$Ru(bpy)_3^{2+}$) by several potential quencher molecules were examined in micellar systems at 77 K. In these systems, pronounced quenching reactivity was observed for *$Ru(bpy)_3^{2+}$ by Cu^{2+}, Cr^{3+}, and Fe(III). At room temperature the mechanism of quenching is known to be an electron-transfer process from *$Ru(bpy)_3^{2+}$ to Cu^{2+} or Fe(III) and an energy-transfer process to Cr^{3+}, in both homogeneous[6] and heterogeneous media[7] (polyelectrolyte, ion-exchange resin, micelle, etc.). For the Py* quenching system, the 1-ethyl-1′-hexadecyl-4,4′-bipyridinium ion showed greater efficiency than other quenchers at room temperature. These emission-quenching reactions will be discussed in terms of their behavior at room temperature and at 77 K.

Experimental Section

Emission-quenching and transient-absorption studies were carried out via a pulsed laser technique using a Lambda Physik EMG-100 excimer laser (λ_{ex} 308 or 337.1 nm; pulse width 6 ns; 100 mJ/pulse), a Photochemical Research Associates nitrogen laser (λ_{ex} 337.1 nm; pulse width 120 ps; 50 μJ/pulse), and a Candela dye laser (λ_{ex} 490 nm; pulse width 120 ns; 50 mJ/pulse). The emission or absorption signals, monitored by an RCA 1P28 photomultiplier tube, were fed into a Tektronix 7912 AD programable digitizer and displayed on a Tektronix 546B storage oscilloscope. All data were analyzed on a Tektronix 4051 or 4052 computer which was interfaced to the digitizer for rapid data reduction. The emission decay curves were fitted to a high degree of precision; i.e., $\sigma <$ 0.0006 over the 512 points of the decay curve, where,

$$\sigma = \frac{1}{N}\left\{\sum_{i=1}^{N}\left[\frac{E(i)}{E(t=0)}(\text{obsd}) - \frac{E(i)}{E(t=0)}(\text{calcd})\right]^2\right\}^{1/2}$$

Absorption and emission spectra were recorded on a Perkin-Elmer 522 spectrophotometer and a Perkin-Elmer MPF-44B fluorescence spectrophotometer, respectively.

Time-dependent luminescence decays were monitored at 400 nm for pyrene, both at room temperature and at 77 K. On the other hand, for the $Ru(bpy)_3^{2+}$ system, luminescence was observed at 610 nm, at room temperature, and at 580 nm, at low temperature, the λ_{max} of the emission spectrum at the two different temperatures.

Sodium lauryl sulfate (BDH, specially pure), ethylene glycol (Fisher), tris(2,2′-bipyridine)ruthenium(II) chloride (Frederik Smith), 9-methylanthracene (Eastman), $CuSO_4$ (Baker), $Fe(ClO_4)_3$ (Frederik Smith), $CrCl_3$ (Fisher), $EuCl_3$ (Alfa Inorganics), and uranyl acetate (Baker) were used as received. Pyrene (Sigma) was recrystallized three times from ethanol, cetylpyridinium chloride was recrystallized three times from an ethanol–ether mixture, and methylviologen chloride (Aldrich) was recrystallized three times from water. 1-Ethyl-1′-hexadecyl-4,4′-bipyridinium bromide was prepared according to the literature[8] in our laboratory and *N,N′*-dimethylaniline (Matheson Coleman & Bell) was vacuum distilled. Distilled and deionized water was used throughout the experiments.

The NaLS micellar solution was usually prepared in a 45% v/v ethylene glycol–water mixture unless otherwise stated.

Nitrogen bubbling was undertaken to purge oxygen for experiments at room temperature (20 ± 1 °C). However, for measurements at 77 K, a degassing procedure was not carried out, since it was confirmed that the lifetimes of both Py* and *$Ru(bpy)_3^{2+}$ were identical in air and N_2 saturated solutions at low temperature.

In the quenching experiment of *$Ru(bpy)_3^{2+}$ by Fe(III), $Fe(ClO_4)_3$ solutions, 1 M in HCl, were rapidly mixed with NaLS–EGW solutions containing $Ru(bpy)_3^{2+}$, followed by immediate cooling in liquid nitrogen.

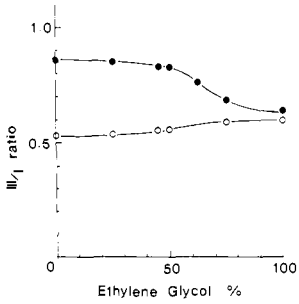

Figure 1. III/I ratio of pyrene fluorescence vs. the volume percent of ethylene glycol in water: (●) in the presence of 0.1 M NaLS; (○) in the absence of NaLS.

Table I. Emission Parameters of Singlet Pyrene and *$Ru(bpy)_3^{2+}$ at Different Environments

	H_2O	EGW[a]		NaLS[b]	NaLS-EGW[c]	
	20 °C	20 °C	77 K	20 °C	20 °C	77 K
III/I(pyrene)[d]	0.53	0.55	0.41	0.86	0.84	0.56
τ_f(pyrene)[e]	220	320	500	400	400	580
τ_E(Ru(II))[f]	700	850	4900	950	940	6000
λ_{max}^{Em}(Ru(II))[g]	614	614	575, 620	628	624	575, 620

[a] Ethylene glycol–water mixture (45% v/v). [b] 0.10 M NaLS in aqueous solution. [c] 0.10 M NaLS in ethylene glycol–water mixture (45% v/v). [d] The III/I ratio of pyrene fluorescence. [e] Fluorescence lifetime (in nanosecond) of pyrene. Errors: 3% at room temperature; 5% at 77 K. [f] Emission lifetime (in nanosecond) of *$Ru(bpy)_3^{2+}$. Errors: 3% at room temperature; 5% at 77 K. [g] Maximum wavelengths of the *$Ru(bpy)_3^{2+}$ emission spectrum.

(1) (a) Fendler, J. H.; Fendler, E. J. "Catalysis in Micellar and Macromolecular Systems"; Academic Press: New York, 1975. (b) Kalyanasundaram, K. *Chem. Soc. Rev.* **1978**, *7*, 453. (c) Turro, N. J.; Grätzel, M.; Braun, A. M. *Angew Chem., Int. Ed. Engl.* **1980**, *19*, 675. (d) Thomas, J. K. *Chem. Rev.* **1980**, *80*, 283.

(2) (a) Henglein, A. *Ber. Bunsenges. Phys. Chem.* **1975**, *79*, 129. (b) Grätzel, M.; Henglein, A.; Janata, E. *Ibid.* **1975**, *79*, 475. (c) Frank, A. J.; Grätzel, M.; Henglein, A.; Janata, E. *Ibid.* **1976**, *80*, 295.

(3) For example: (a) Dederen, J. C.; Van der Auweraer, M.; De Schryver, F. C. *Chem. Phys. Lett.* **1979**, *68*, 451. (b) Moroi, Y.; Infelta, P. P.; Grätzel, M. *J. Am. Chem. Soc.* **1979**, *101*, 573. (c) Hatlee, M. D.; Kozak, J. J.; Rothenberger, G.; Infelta, P. P.; Grätzel, M. *J. Phys. Chem.* **1980**, *84*, 1508. (d) Tachiya, M. *J. Chem. Phys.* **1982**, *76*, 340.

(4) (a) Narayana, P. A.; Li, A. S. W.; Kevan, L. *J. Am. Chem. Soc.* **1981**, *103*, 3603. (b) Narayana, P. A.; Li, A. S. W.; Kevan, L. *J. Phys. Chem.* **1982**, *86*, 3.

(5) For example: (a) Miller, J. R. *J. Chem. Phys.* **1972**, *56*, 5173. (b) Miller, J. R. *Chem. Phys. Lett.* **1973**, *22*, 180. (c) Miller, J. R.; Beitz, J. V. In "Proceedings of the Sixth International Congress of Radiation Research"; Japanese Association for Radiation Research: Tokyo, 1979. (d) Beitz, J. V.; Miller, J. R. *J. Chem. Phys.* **1979**, *71*, 4579.

(6) (a) Bock, C. R.; Meyer, T. J.; Whitten, D. G. *J. Am. Chem. Soc.* **1974**, *96*, 4710. (b) Lin, C-T.; and Sutin, N. *Ibid.* **1975**, *97*, 3543. (c) Lin, C-T.; Böttcher, W.; Chou, M.; Creutz, C.; Sutin, N. *Ibid.* **1976**, *98*, 6536. (d) Meisel, D.; Matheson, M. S.; Mulac, W. A.; Rabani, J. *J. Phys. Chem.* **1977**, *81*, 1449. (e) Hoselton, M. A.; Lin, C-T; Shwartz, H. A.; Sutin, N. *J. Am. Chem. Soc.* **1978**, 100, 2383.

(7) (a) Meisel, D.; Matheson, M. S. *J. Am. Chem. Soc.* **1977**, *99*, 6577. (b) Meyerstein, D.; Rabani, J.; Matheson, M. S.; Meisel, D. *J. Phys. Chem.* **1978**, *82*, 1879. (c) Meisel, D.; Matheson, M. S.; Rabani, J. *J. Am. Chem. Soc.* **1978**, *100*, 117. (d) Thornton, A. T.; Laurence, G. S. *J. Chem. Soc., Chem. Commun.* **1978**, 408. (e) Jonah, C. D.; Matheson, M. S.; Meisel, D. *J. Phys. Chem.* **1979**, *83*, 257. (f) Lee, P. C.; Meisel, D. *J. Am. Chem. Soc.* **1980**, *102*, 5477. (g) Slama-Schwok, A.; Feitelson, Y.; Rabani, J. *J. Phys. Chem.* **1981**, *85*, 2222.

(8) Takuma, K.; Sakamoto, T.; Nagamura, T.; Matsuo, T. *J. Phys. Chem.* **1981**, *85*, 619.

This was done to minimize the hydrolysis of NaLS in acidic solution. This rapid mixing and freezing method was also applied to the Ru(bpy)$_3^{2+}$–UO_2^{2+} system (pH 2).

Results and Discussion

A. Micellar Formation of NaLS in Ethylene Glycol–Water Mixtures. 1. At Room Temperature. The III/I ratio of pyrene fluorescence, which is the ratio of the third and first vibronic bands, is known to be sensitive to the environment in which the molecule resides.[9] Figure 1 shows the III/I ratio of pyrene in an ethylene glycol–water mixture (EGW) both in the presence and in the absence of 0.10 M sodium lauryl sulfate (NaLS). In the absence of NaLS, at any ratio of ethylene glycol and water, the III/I ratio undergoes only a slight change showing the polar nature of this mixed solvent. However, in a solution containing 0.10 M NaLS, the III/I ratio changed markedly from 0.86 in pure aqueous solution, where pyrene is known to reside inside the micelle, to 0.64 in pure ethylene glycol solution. Up to at least 50% v/v of ethylene glycol, the ratio has a similar value to that in normal aqueous micellar solution. These data suggest that micellar structures occur in an EGW solution below 50% v/v of ethylene glycol. Several investigations[10] have already shown that micellar structures exist in the presence of alcohols in spite of the changes in their physical parameters (e.g., cmc, aggregation number, etc.). Table I compares the emission spectroscopic parameters of the luminescent probes pyrene and tris(2,2′-bipyridine)ruthenium(II) (Ru(bpy)$_3^{2+}$) in water, ethylene glycol–water mixtures (45% v/v), a 0.10 M NaLS aqueous solution (NaLS solution), and a 0.10 M NaLS in 45% EGW solution (NaLS–EGW solution). Both singlet excited pyrene and *Ru(bpy)$_3^{2+}$ in a NaLS–EGW solution have the same lifetimes as those observed in NaLS solution. These are larger than those observed in water or EGW mixtures. It was also noted that pyrene, solubilized in a 0.10 M NaLS–EGW solution, was not efficiently quenched by I^- ions. This is similar behavior to that observed in a 0.10 M NaLS solution (i.e., the lifetime of pyrene fluorescence in the presence of 1.0×10^{-2} M NaI, both in 0.10 M NaLS solution and 0.10 M NaLS–EGW solution, is 380 ns). In EGW solution, pyrene was efficiently quenched by I^-, with $k_q = 2.9 \times 10^8$ M^{-1} s^{-1}. These results also indicate that micelles are formed in a NaLS–EGW solution.

More accurate features of micelles in a NaLS–EGW solution were obtained from the determination of the cmc (critical micellar concentration) and aggregation number. The cmc was measured by observing the III/I ratio of pyrene fluorescence, a technique which has previously been shown to give the correct estimation of the cmc for aqueous micellar solutions.[9b] Decreasing the NaLS concentration from 0.10 M in 45% v/v EGW solutions causes a sudden reduction in the pyrene fluorescence III/I ratio at between 2.2×10^{-2} M and 2.0×10^{-2} M NaLS. Thus, we determined the cmc of NaLS in an EGW solution as 2.1×10^{-2} M. The value is three times larger than that in aqueous solution (8.0×10^{-3} M[11a] or 8.2×10^{-3} M[11b]). This method was simultaneously checked by the estimation of cmc of NaLS in water, which gave 7.5×10^{-3} M.

The aggregation number ($\bar{N}$) was determined by analysis of time-resolved luminescence quenching of *Ru(bpy)$_3^{2+}$ by 9-methylanthracene (9-MA). The method, originally proposed by Turro and Yekta[12a] for steady-state quenching studies, was later successfully applied to time-dependent emission decay in a NaLS micellar system by Almgren et al.[10a] and Rogers et al.[12b] For application of the Turro and Yekta method, it is necessary that Ru(bpy)$_3^{2+}$ and 9-MA are on, or in, the micelle. In normal NaLS micelles, it has been demonstrated that practically all of the added Ru(bpy)$_3^{2+}$ attaches to the micellar surface, which causes a red shift in the emission peak due to interaction between the Ru(II) complex and hydrocarbon chains.[6d] The maximum wavelength of the *Ru(bpy)$_3^{2+}$ emission in an EGW solution was the same as that in water, indicating an environment of equal polarity. The red shift of the emission peak observed in a NaLS–EGW solution must be due to interaction between Ru(bpy)$_3^{2+}$ and micelles. In a NaLS–EGW solution, the micellar structure would be one where ethylene glycol molecules may insert themselves among surfactant molecules in a similar fashion to alcohols in microemulsion systems. Thus the environment of Ru(bpy)$_3^{2+}$ in a NaLS–water and NaLS–EGW solutions should be different, and accounts for the small red shift observed in a NaLS–EGW solution. Consequently, in NaLS–EGW solution, Ru(bpy)$_3^{2+}$ is strongly bound to the micellar surface by Coulombic interaction. It is interesting to note the macroscopic observation of precipitation which was observed for NaLS–EGW solutions below cmc by the addition of Ru(bpy)$_3^{2+}$ did not occur at concentrations of NaLS > cmc. This behavior bears a close resemblance to purely aqueous NaLS solutions as described by Meisel et al.[6d] The low solubility of 9-MA in an EGW solution, as in water, also supports the assumption that 9-MA resides with the micelles in the NaLS–EGW solution. The 308-nm line from an excimer laser was used as an excitation source in these experiments. The 308-nm line is only weakly absorbed by 9-MA compared to Ru(bpy)$_3^{2+}$, i.e., ϵ(308 nm) = 1.6×10^4 M^{-1} cm^{-1} for Ru(bpy)$_3^{2+}$ and ϵ(308 nm) = 940 M^{-1} cm^{-1} in the NaLS solution, practically the same values as in the NaLS–EGW solution. Figure 2, parts A and B, depicts the time-resolved luminescence decay of *Ru(bpy)$_3^{2+}$ in the presence of 9-MA. Without 9-MA, the luminescence decay followed a single exponential function. The curves were analyzed by the well-known equation[13]

$$F(t) = F(0) \exp\{(-t/\tau_0) + \bar{n}(e^{-k_q t} - 1)\} \quad (1)$$

where τ_0 is the unquenched lifetime, $\bar{n} = [Q]/[M]$, and k_q is the first-order rate constant for the luminescence quenching in a

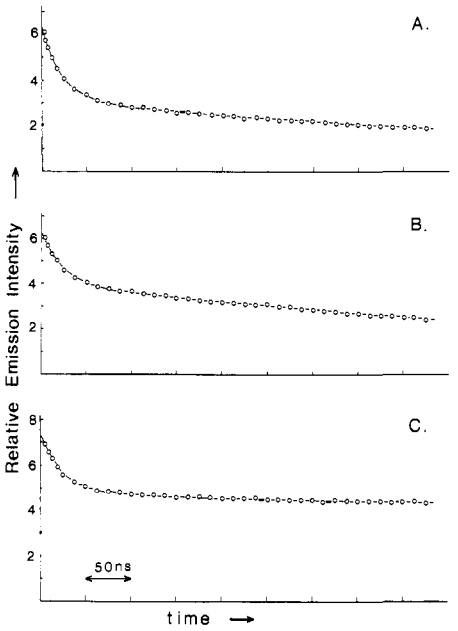

Figure 2. Time-dependent emission decay of *Ru(bpy)$_3^{2+}$ in the presence of 9-methylanthracene. [Ru(bpy)$_3^{2+}$] = 5.7×10^{-5} M, (A) 0.050 M NaLS aqueous micellar solution at room temperature, [9-MA] = 4.3×10^{-4} M, $1/\tau_0 = 1.2 \times 10^6$ s^{-1}, $k_2 = 4.0 \times 10^7$ s^{-1}, $\bar{n} = 0.68$. (B) 0.050 M NaLS in a 45% ethylene glycol–water mixture at room temperature, [9-MA] = 4.4×10^{-4} M, $1/\tau_0 = 1.2 \times 10^6$ s^{-1}, $k_2 = 4.0 \times 10^7$ s^{-1}, $\bar{n} = 0.43$, (C) 0.050 M NaLS in an EGW solution at 77 K, [9-MA] = 4.4×10^{-4} M, $1/\tau_0 = 1.8 \times 10^5$ s^{-1}, $k_2 = 4.0 \times 10^7$ s^{-1}, $\bar{n} = 0.43$.

(9) (a) Nakajima, A. *Bull. Chem. Soc. Jpn.* **1971**, *44*, 3271. (b) Kalyanasundaram, K.; Thomas, J. K. *J. Am. Chem. Soc.* **1977**, *99*, 2039.

(10) (a) Almgren, M.; Löfroth, J.-E. *J. Colloid Interface Sci.* **1981**, *81*, 486. (b) Backlund, S.; Rundt. K.; Birdi, K. D.; Dalsager, S. *Ibid.* **1981**, *79*, 578. (c) Grieser, F. *J. Phys. Chem.* **1981**, *85*, 928.

(11) (a) Mukerjee, P.; Mysels, K. J. "Critical "Nonionic Concentrations of Aqueous Surfactant Systems", *Natl. Stand. Ref. Data Ser.* (U.S. *Natl. Bur. Stand*) **1971**, *No. 36*. (b) Hall, D. G.; Pethica, B. A. "Nonionic Surfactants"; Schick, M. J., Ed.; Marcel Dekker: New York, 1967.

(12) (a) Turro, N. J.; Yekta, A. *J. Am. Chem. Soc.* **1978**, *100*, 5951. (b) Rogers, M. A. J.; Baxendale, J. H. *Chem. Phys. Lett.* **1981**, *81*, 347.

(13) For example: Yekta, A.; Aikawa, M.; Turro, N. J. *Chem. Phys. Lett.* **1979**, *63*, 543 and references cited therein.

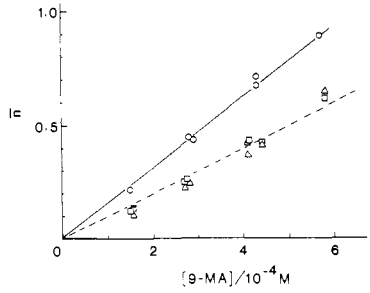

Figure 3. Calculated $\bar{n}$ as a function of the concentration of 9-methylanthracene: (○) in 0.050 M NaLS aqueous solution at room temperature; (□) 0.050 M NaLS–EGW solution at room temperature; (△) 0.050 M NaLS–EGW solution at 77 K.

micelle containing one quencher. Direct fitting of the decay curves by eq 1 with use of the experimentally obtained τ_0 and parameters $\bar{n}$ and k_q was performed. $\bar{n}$ was plotted against the quencher concentration, 9-MA, as shown in Figure 3. Then aggregation number, $\bar{N}$, was calculated according to the equation

$$\bar{n} = \frac{[Q]}{([NaLS] - cmc)/\bar{N}} \qquad (2)$$

using the slope $\bar{n}/[Q]$ in Figure 3, [NaLS] = 0.050 M, and cmc = 2.1×10^{-2} M. The value obtained for $\bar{N}$ in a 0.050 M NaLS–EGW solution is 29 ± 2. This value is almost one-half that obtained for NaLS in aqueous solution. The simultaneously estimated $\bar{N}$ for 0.050 M NaLS solution, 66 ± 4, gives good agreement with Turro's 60 ± 2[12a] or 62[14a] and 63,[14b] estimated utilizing other methods. This is taken as an indication of the reliability of the results. It is pertinent to point out that addition of alcohols to aqueous micellar solutions is known to cause a decrease in aggregation number.[10]

2. Surfactant Solutions at 77 K. EGW solutions (45% v/v) of surfactant molecules (NaLS, cetyltrimethylammonium bromide (CTAB), cetylpyridinium chloride (CPCl)) form glasses at liquid nitrogen temperature of 77 K. At surfactant concentrations below 0.07 M, the glasses formed are almost optically transparent, at 0.1 M translucent, and at 0.2 M nearly opaque.

The excited singlet state of pyrene (Py*) or the lowest charge-transfer excited state of $Ru(bpy)_3^{2+}$ ($*Ru(Bpy)_3^{2+}$) have appreciably longer lifetimes in a 0.10 M NaLS–EGW solution than in an EGW solution (Table I). The III/I ratio of the pyrene fluorescence is substantially reduced at 77 K compared to that at room temperature (Table I). This was also the case in other solvents: e.g., in 3-methylpentane, where III/I is 1.73 at room temperature and 1.19 at 77 K; in an ethanol–methanol (4:1 v/v) mixture III/I is 0.78 at room temperature and 0.51 at 77 K. It is noteworthy that the III/I ratio in an ethanol–methanol mixture, an environment for pyrene at room temperature that is expected to be similar to that in an NaLS micelle at 77 K, was similar to that obtained in a NaLS–EGW solution at 77 K; the values are larger than the III/I ratio in an EGW solution. The results of the lifetime data and the III/I ratios are insufficient in themselves to conclusively verify micellar formation. However, the method utilizing the quenching of $*Ru(bpy)_3^{2+}$ by 9-MA provides additional proof, at 77 K.

As shown in Figure 2C, $*Ru(bpy)_3^{2+}$ is quenched by 9-MA. An initial fast decay is observed by time-resolved luminescence, which is accompanied by a subsequent very slow component, which decays according to an exponential function, whose decay constant is the reciprocal of the unquenched lifetime. These data are understood with the assumption that micelles are formed in the glassy solution, and that 9-MA is distributed among the micelles obeying Poisson statistics in the room-temperature system. However, quenching only takes place in micelles which contain both probe and quencher. Therefore, a kinetic analysis using eq 1 was undertaken in order to estimate the aggregation number

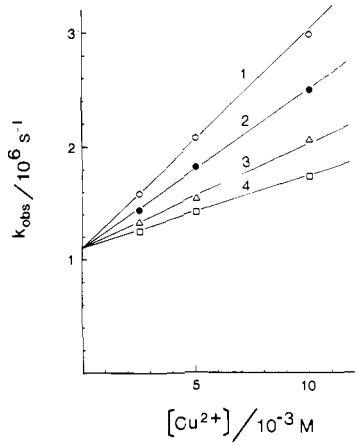

Figure 4. k_{obsd} vs. the concentration of Cu^{2+} at different NaLS concentrations in an EGW solution: (1) 0.050 M NaLS; (2) 0.070 M NaLS; (3) 0.10 M NaLS; (4) 0.15 M NaLS; $1/\tau_0 = 1.1 \times 10^6\ s^{-1}$.

at 77 K. The aggregation number, $\bar{N} = 29 \pm 4$, was essentially the same as that obtained at room temperature. This strongly suggests that similar micellar structures occur at room temperature and at 77 K in NaLS–EGW solutions. Furthermore, the observed first-order quenching kinetics at 77 K has an important meaning, because it suggests that quenching takes place with a narrow distribution of separations for the quenchee–quencher pairs: if the quencher molecules were distributed at random distances from the probes, then the luminescence decay should show unusual features as described by Inokuti and Hirayama.[15] A simple spherical micellar structure model is also useful in explaining the fixed energy-transfer distance observed at 77 K in NaLS–EGW solutions.

B. Luminescence-Quenching Reaction in Micellar Systems at 77 K. It is now possible to state with some confidence that micellar formation at 77 K in EGW mixtures actually occurs, and that these systems may be used to study reactions of interest. One of the interesting features of the NaLS–EGW micellar system is that pyrene excimer emission, which is observed at room temperature in a 0.1 M NaLS–EGW solution containing 1×10^{-3} M pyrene, nevertheless completely disappears on cooling to 77 K. This indicates prohibition of diffusional motion of pyrene molecules at that temperature. The following section discusses the occurrence of certain but unusual luminescence-quenching reactions, which further prove the presence of micelles, and the retention of their intrinsic nature at 77 K, and compares the data to those at room temperature.

1. Quenching of $*Ru(bpy)_3^{2+}$ by Cu^{2+}, Cr^{3+}, and Fe(III). Many investigations have claimed that Cu^{2+} is an efficient oxidative quencher of the excited state of $Ru(bpy)_3^{2+}$ both in homogeneous[6d,e] and heterogeneous[7a,c,d,f,g] systems, including micelles at room temperature. Observations of the *Ru(II) emission quenching (λ_{ex} 337 nm) by Cu^{2+} in a NaLS–EGW micellar solution exhibit psuedo-first-order kinetics in the surfactant range 0.050–0.15 M NaLS, and the decay constant, k_{obsd}, was found to be linear with Cu^{2+} concentration as shown in Figure 4. This quenching behavior is quite similar to that observed for this quenchee–quencher system in a NaLS micellar solution.[16b] As has already been discussed in some detail, this type of quenching behavior can be understood by a mechanism whereby the quenching process is sufficiently slow so as to allow equilibration of quenchers among the micelles. By treating the data in exactly the same way as Grieser et al.[16a] or Baxendale et al.,[16b] we obtained an equilibrium constant (K_A) for Cu^{2+} between solvent medium and micellar surface of $K_A = 1.8 \times 10^3\ M^{-1}$ and a first-order quenching rate constant (k_q) for Cu^{2+} on micelles of $k_q = 3.2 \times 10^5\ s^{-1}$. This k_q value compares with the value $2.1 \times 10^5\ s^{-1}$ in

(14) (a) Granath, K. *Acta Chem. Scand.* **1953**, *7*, 297. (b) Coll, H. *J. Phys. Chem.* **1970**, *74*, 520.

(15) Inokuti, M.; Hirayama, F. *J. Chem. Phys.* **1965**, *43*, 1978.

(16) (a) Grieser, F.; Tausch-Treml, R. *J. Am. Chem. Soc.* **1980**, *102*, 7258. (b) Atherton, S. J.; Baxendale, J. H.; Hoey, B. M. *J. Chem. Soc., Faraday Trans. 1* **1982**, *78*, 2167. (c) Dederen, J. C.; Van der Auweraer, M.; and De Schryver, F. C. *J. Phys. Chem.* **1981**, *85*, 1198.

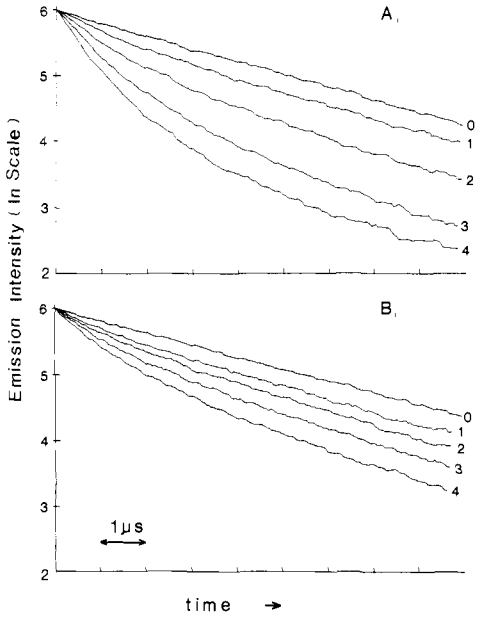

Figure 5. ln plot of the time-dependent emission decay of $*Ru(bpy)_3^{2+}$ at 77 K in the presence of Cu^{2+}, $[Ru(bpy)_3^{2+}] = 5.7 \times 10^{-5}$ M: $[Cu^{2+}]$, (0) 0 M, (1) 1.25×10^{-3} M; (2) 2.5×10^{-3} M; (3) 5.0×10^{-3} M; (4) 1.0×10^{-2} M. (A) In 0.070 M NaLS–EGW solution. (B) In 0.15 M NaLS–EGW solution.

a NaLS micellar solution determined by Baxendale et al.[16a] On the other hand, K_A is at least one order of magnitude smaller than that in a NaLS solution which is 1.0×10^4 M^{-1},[16c] 2.0×10^4 M^{-1},[16b] or 6.0×10^4 M^{-1}.[16a] The reduction of K_A in a NaLS–EGW solution compared to a NaLS solution can be explained by decreased charge density of the micellar surface caused by a lowering of the ionization constant of NaLS in an EGW solution, and/or by the spacing of ethylene glycol molecules among surfactants. The close similarity of the quenching reaction of $*Ru(bpy)_3^{2+}$ by Cu^{2+} at room temperature in the NaLS–EGW solution to that in a NaLS solution supports the contention that the present system behaves much like normal micelles in luminescence-quenching reactions.

Emission quenching of $*Ru(bpy)_3^{2+}$ by Cu^{2+} was observed in a NaLS–EGW glassy micellar solution at 77 K (λ_{ex} 337 nm).[17] Figure 5, parts A and B, show that the time-dependent luminescence decay of *Ru(II) depends upon both the quencher concentration over the range from 1.25×10^{-3} to 1.0×10^{-2} M and the surfactant concentration from 0.050–0.15 M. Both the Ru(II) complex and the quencher are generally considered to be bound to the surface of micelles at 77 K; this is the case at room temperature, and the micellar structures are similar at room temperature and at 77 K. It should be pointed out that the quenching of excited states of $Ru(bpy)_3^{2+}$ (the same concentration as in a NaLS–EGW solution) by Cu^{2+} (2.0×10^{-2} M) in an EGW homogeneous glassy solution does not occur. This shows that the observed quenching reaction could only take place between positively charged quenchee and quencher adsorbed on the negatively charged micellar surface. It seems quite reasonable to assume that the diffusional motion of the Ru(II) complex and the quencher are highly prohibited in the system at 77 K. As shown in Figure 5, the time-dependent decay of the $*Ru(bpy)_3^{2+}$ emission in the presence of Cu^{2+} at 77 K is quite different from that at room temperature. Unusual quenching kinetics are observed, which obey neither the first-order nor the second-order process.

The quenching of $*Ru(bpy)_3^{2+}$ luminescence by Fe(III) (in this work Fe(III) will represent the sum of all ferric forms under the given conditions (pH 2.0)) and by Cr^{3+} was also observed in the NaLS–EGW micellar system at 77 K. No quenching is observed in the relevant EGW glassy solutions (λ_{ex} of $*Ru(bpy)_3^{2+}$ is 490 nm for Fe(III) and 337 nm for Cr^{3+}). It is pertinent to note that we failed to observe quenching by the potential quenchers nitrobenzene, *N,N'*-dimethylaniline (DMA), methylviologen (MV^{2+}), Ag^+, Eu^{3+}, duroquinone, and UO_2^{2+}.

The observed quenching may proceed by an energy-transfer from or oxidative electron transfer of the excited Ru(II) complex. Transient absorption studies were carried out in the present $Ru(bpy)_3^{2+}$–Cu^{2+} system in a 0.050 M NaLS–EGW solution both at room temperature and at low temperature (λ_{ex} 337 nm). At room temperature, the decay of the bleaching at 460 nm exhibited two stages in the presence of 1.0×10^{-2} M Cu^{2+}: an initial fast component that decayed more rapidly than the bleaching in the absence of the quencher, followed by a slower decay that is considered to correspond to the back electron transfer

$$Ru(bpy)_3^{3+} + Cu^+ \rightarrow Ru(bpy)_3^{2+} + Cu^{2+}$$

The slower component exhibited a slower decay than that in the absence of quencher. However, at 77 K, the bleaching decay at 460 nm in the presence of 1.0×10^{-2} M Cu^{2+} exhibits similar kinetics to the decay of the absorption at 360 nm due to $*Ru(bpy)_3^{2+}$[18] or that of luminescence at 580 nm: a faster decay compared with the nonquencher system was observed, but no evidence of two-stage behavior of the bleaching decay, which might be indicative of electron transfer, was obtained.

The recent works by Sutin et al.[6c,e] have rationalized the quenching mechanism of the *Ru(II) complex by metal ions from the free-energy dependence upon the quenching rate constant k_q in homogeneous solution at room temperature. According to their work, the quenching by Cr^{3+} is ascribable to energy transfer in which the $(t_{2g})^2(e_g)$ and/or $(t_{2g})^3$ excited states of Cr^{3+} (2.16 and 1.86 eV, respectively) are produced. On the other hand, the mechanism of the quenching by Cu^{2+} or Fe^{3+} is predominantly electron transfer, although the ions have an energy level which could act as an acceptor (the $(t_{2g})^5(e_g)^4$ excited state of Cu^{2+} lies about 1.55 eV and the $(t_{2g})^4(e_g)$ state of Fe^{3+} is about 1.5 eV above the ground state). It is quite reasonable to conclude that energy transfer is operative for the Cr^{3+} quenching in the present system: Cr^{3+} ($E^0(Cr^{3+}/Cr^{2+}) = -0.41$ V) is not as strong an oxidant as Cu^{2+} or Fe^{3+} ($E^0(Cu^{2+}/Cu^+) = +0.15$ V and $E^0(Fe^{3+}/Fe^{2+}) = +0.74$ V), and energy transfer to Cr^{3+} from $*Ru(bpy)_3^{2+}$ (2.12 eV) has been observed in homogeneous medium at room temperature.[6c] Furthermore, MV^{2+} and Eu^{3+}, which have similar reduction potentials ($E^0(MV^{2+}/MV^+) = -0.45$ V and $E^0(Eu^{3+}/Eu^{2+}) = -0.43$ V) to that of Cr^{3+}, and are the oxidative quencher of the *Ru(II) complex in homogeneous solution at room temperature,[6c,19] nevertheless did not quench $*Ru(bpy)_3^{2+}$ in a NaLS–EGW micelle at 77 K. The result of transient absorption measurement mediates against an electron-transfer mechanism for quenching by Cu^{2+} at 77 K. This is also supported by the fact that UO_2^{2+} failed to quench the excited state of $Ru(bpy)_3^{2+}$ in our system at 77 K (at pH 2).[20] The reduction potential of UO_2^{2+}, $E^0(UO_2^{2+}/UO_2^{+}) = +0.06$ V, is comparable to that of Cu^{2+}. Therefore, energy transfer seems to be more likely for the Cu^{2+} quenching. The dominant mechanism of the quenching by Fe(III) cannot be decided here; further discussion will be given below.

The analysis of the decay curves for the quenching experiments was based on the model which takes into consideration a distribution distance for the quenchee–quencher pairs participating in the quenching reaction: the quenching phenomena are due to energy transfer or electron transfer to quenchers, which are randomly distributed around the probe molecules. If energy transfer or electron transfer of this type occurs, and competes with natural emission decay with a lifetime of τ_0, then the time-de-

(17) The addition of Cu^{2+} caused neither a change in the shape of the absorption spectrum of $Ru(bpy)_3^{2+}$ nor in that of the emission spectrum, even at 77 K. And, the time-dependent emission decay of $*Ru(bpy)_3^{2+}$ in the presence of Cu^{2+} was not affected at different wavelengths of the spectrum.

(18) Bensasson, R.; Salet, C.; Balzani, V. *J. Am. Chem. Soc.* **1976**, *98*, 3722.

(19) Rogers, M. A. J.; Becker, J. C. *J. Phys. Chem.* **1980**, *84*, 2762.

(20) The substantial quenching of $*Ru(bpy)_3^{2+}$ by UO_2^{2+} in aqueous solution (at pH 2.0) was observed at room temperature. See: Rosenfeld-Grunwald, T.; Rabani, J. *J. Phys. Chem.* **1980**, *84*, 2981.

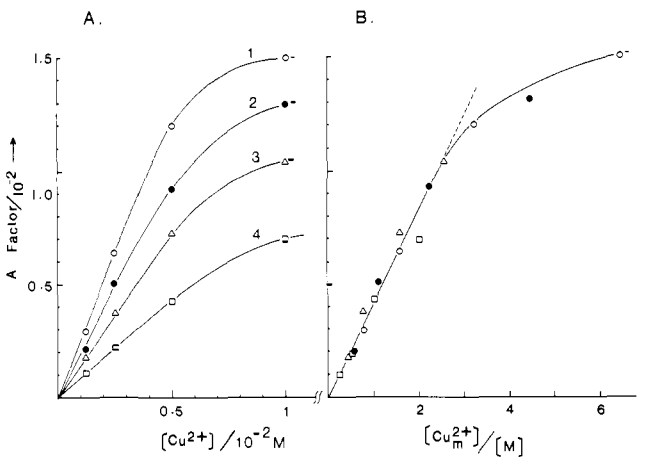

Figure 6. (A) Calculated A factors against the Cu^{2+} concentration at different NaLS concentrations: (1) 0.050 M NaLS; (2) 0.070 M NaLS; (3) 0.10 M NaLS; (4) 0.15 M NaLS. (B) Calculated A factors against the average occupation number of Cu^{2+} per micelle, $[Cu_m^{2+}]/[M]$: (○) 0.050 M NaLS; (●) 0.070 M NaLS; (△) 0.10 M NaLS; (□) 0.15 M NaLS.

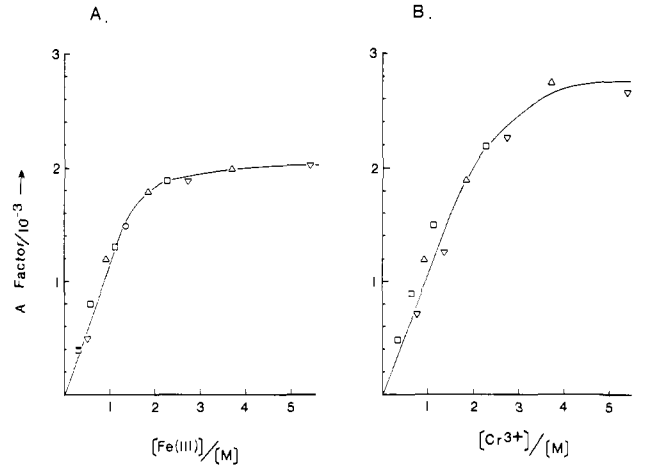

Figure 7. Calculated A factors against the average number of quenchers per micelle, $[Q]/[M]$. Data points are from different NaLS concentrations: (▽) 0.075 M NaLS; (△) 0.10 M NaLS; (□) 0.15 M NaLS. (A) Fe(III) as a quencher. (B) Cr^{3+} as a quencher.

pendent decay of the $*Ru(bpy)_3^{2+}$ luminescence can be described by:

$$F(t) = F(0)\exp\{(-t/\tau_0) - A(\ln \omega t)^3\} \quad (3)$$

where ω is a constant which is related to the first-order rate constant $k(r)$ by

$$k(r) = \omega \exp(-2r/L) \quad (4)$$

in which r is the donor-acceptor distance and L is a positive constant, and A is a linear function of acceptor concentration C_s:

$$A = (\text{constant})C_s \quad (5)$$

The detailed expression concerning ω or A has been given in the literature both for the energy transfer[15] and for the electron transfer.[5c,d,21] The second term of eq 3 is the same as the simplest version of the formula which expresses Dexter-type energy transfer from excited donor to the randomly distributed acceptors in the system where the translational motion of all the solutes is too slow to occur. The formula was originally introduced by Inokuti and Hirayama[15] to explain kinetics of donor luminescence decay by the exchange mechanism in a homogeneous rigid solution. It was shown that the formula, which is based on a tunneling hypothesis that an electron in a simple square well potential tunnels to randomly distributed acceptors, is also reduced to the second term of eq 3. This was done originally by Miller[5a,b] and later by Tachiya and Mozumder.[21] In our glassy micellar system, the distribution of solutes is not totally homogeneous. However, the quencher ions are considered to be distributed *randomly* within the limited space of the micellar surface, since it was not necessary to take into consideration the reaction with the quencher residing outside the micelle within the lifetime of the excited species. In addition, the formula or the second term of eq 3 essentially only considers transfer to the nearest scavenger molecule; this is because of the nature of the assumed probability density function, a feature pointed out by Tachiya and Mozumder.[21] Therefore we assumed the same probability density as that of Inokuti and Hirayama's for the distribution of the quencher ions on micelles. (This may not be exact. But we have no precise knowledge of the accurate distribution of ions on a micelle surface.)

As indicated above, C_s in eq 5 should be the concentration of the ions on the micelle. This is estimated from the total concentration of quencher from the following relation

$$[Q_m] = \frac{K_A[Q]}{1 + K_A[M]}[M] \quad (6)$$

where $[Q_m]$ is the concentration of the quencher on the micelles, $[Q]$ is the concentration of added quencher, K_A is the binding constant of quencher and micelle, and $[M]$ is the concentration of micelles. The condition $1/\omega \leq t$ should be satisfied for the application of eq 3 because of the limitations of the approximate equation.[21] Direct fitting of experimental decay curves to eq 3 at various $[Q]$ and $[NaLS]$ was performed for these three quencher systems, while varying the A value and ω value, and with constant τ_0 (the observed unquenched lifetime). Figure 6A shows A values of the Cu^{2+} quenching system obtained for an optimized ω value of 5×10^7 s^{-1}. Figure 6A was constructed as shown in Figure 6B by taking the average occupation number of the quencher per micelle, $[Cu_m^{2+}]/[M]$ (evaluated from eq 6) on the abscissa ($[M]$ was estimated by $[M] = ([NaLS] - cmc)/\bar{N}$). The applicability of eq 3 to the present emission quenching systems is corroborated by the linearity of the A factors against concentration of quencher on micelles, i.e., $[Q_m]/[M]$ according to eq 5. As shown in Figure 6B, this relation holds well over a large range of $[Cu_m^{2+}]/[M]$ regions, despite the leveling off of the A factor which occurs at higher $[Cu_m^{2+}]/[M]$. From a consideration of the $*Ru(bpy)_3^{2+}$ quenching experiment by Cu^{2+} at room temperature (i.e., the measurement of the binding constant of Cu^{2+} on micelle), $[Cu_m^{2+}]/[M] = 4$ or 5 seems to be far from the saturation of Cu^{2+} binding on micelles. However, it is also likely that the concentration of Cu^{2+} at $[Cu_m^{2+}]/[M] = 4$–5 is such that most of the closer positions (or region) to the Ru(II) complex on micelles, i.e., the sites being effective for emission quenching, are occupied, and further addition of Cu^{2+} may be ineffective. Figure 7, parts A and B, represent the A values at different quencher numbers per micelle, $[Q]/[M]$ for Fe(III) and Cr^{3+} quenching systems, respectively. $[Q]/[M]$ was employed instead of $[Q_m]/[M]$ on the abscissa in Figure 7 because no K_A are available for Fe(III) or Cr^{3+} binding to micelles. (This assumption corresponds to an infinite value for K_A according to eq 6, and may be expected from the high valency of these ions.) The optimized ω value was 5×10^8 s^{-1} for the Fe(III) system, and 2×10^8 s^{-1} for the Cr^{3+} system. The dependence of A factors on the quencher numbers per micelle both for the Fe(III) and for the Cr^{3+} system has a trend analogous to the Cu^{2+} quenching system: The A factor is initially linear against $[Q]/[M]$ and then levels off at higher values of $[Q]/[M]$.[22] Therefore, it can be concluded that eq 3 is applicable for the present emission quenching kinetics at least at rather low quencher concentrations. As was indicated by eq 4, the meaning of the ω value is equivalent to a first-order quenching constant by energy (or electron) transfer.

For the energy transfer mechanism, ω is also expressed by

$$\omega = \frac{2\pi}{h}K^2 \int f_D(E)F_A(E)\,dE \quad (7)$$

(21) Tachiya, M.; Mozumder, A. *Chem. Phys. Lett.* **1974**, *28*, 87.

(22) The leveling off of the A factors with concentration may be indicative of very short-range quenching by the exchange mechanism.

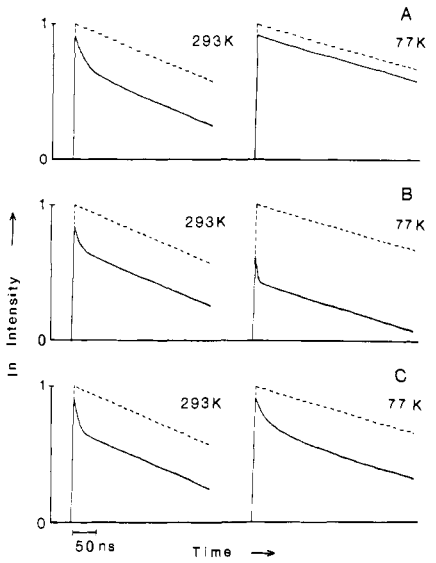

Figure 8. Pictorial representations of time-dependent fluorescence decay from excited pyrene in a 0.1 M NaLS–EGW solution both at room temperature and at 77 K in the presence of 5×10^{-4} M quencher: (A) cetylpyridinium (CP^+) chloride; (B) methylviologen (MV^{2+}) chloride; (C) 1-ethyl-1′-hexadecyl-4,4′-bipyridinium ($C_{16}C_2V^{2+}$) bromide. Dotted lines show the decay in the absence of quencher.

where K is a constant, $f_D(E)$ is the donor emission spectrum, and $F_A(E)$ is the acceptor absorption spectrum. From eq 7, the absorption spectrum of the quencher in the region of the $*Ru(bpy)_3^{2+}$ luminescence spectrum, i.e., $S(Q)$ (550–700 nm), qualitatively measures the magnitude of ω for the energy-transfer mechanism. The observed order of S was $S(Cr^{3+}) > S(Cu^{2+}) \gg S(Fe(III))$. In fact, Fe(III) has practically no absorption from 500 to 700 nm even at 1.0×10^{-2} M (the highest concentration used). However, the ω value, or rate constant of quenching by Fe(III), is much larger than Cu^{2+} or Cr^{3+} and an energy-transfer mechanism is thus ruled out. The higher value of the reduction potential of Fe(III) compared to that of Cu^{2+} or Cr^{3+} may be the driving force for the $*Ru(bpy)_3^{2+}$ quenching. The A factors obtained for the Cu^{2+} system have much larger values than those for Fe(III) or Cr^{3+} systems. This gives rise to a larger quenching distance for Cu^{2+} than that for Cr^{3+} or Fe(III), i.e., a larger "critical transfer distance" can be obtained for Cu^{2+}. Further discussion concerning the A factor for quenching was not carried out in the present paper due in part to the poor theoretical basis for the analysis of the quenching mechanism, and in part to our insufficient understanding of an accurate micellar structure[23] (size, shape, the situation of the surface, etc.), and of the precise distribution of ions on micelle.

2. Quenching of Singlet Pyrene. Quenching experiments of the pyrene fluorescence by well-established quenchers were studied in NaLS micellar systems in an EGW solution at 77 K. An apparent quenching effect was observed for the surfactant-type viologen derivative, 1-ethyl-1′-hexadecyl-4,4′-bipyridinium ($C_{16}C_2V^{2+}$) ion. At room temperature, the fluorescence decay in the presence of $C_{16}C_2V^{2+}$ showed two-stage behavior, an initial fast stage ascribable to quenching on a micelle followed by a slower one, the decay constant of which was the reciprocal of an unquenched lifetime. The fluorescence decays at 77 K and room temperature in the presence of $C_{16}C_2V^{2+}$ were quite similar although the two-phase nature of the 77 K decay is not so pronounced as that at room temperature. The decay constant becomes that of a non-quenched system at sufficiently long time (300 ns–1 μs).

For an understanding of $C_{16}C_2V^{2+}$ quenching, comparison was made for this system with quenching phenomena for singlet pyrene by the methylviologen (MV^{2+}) ion and by the amphiphilic molecule cetylpyridinium (CP^+) ion. Figure 8, parts A, B, and C, depicts typical features of the fluorescence decay in the presence of CP^+, MV^{2+}, and $C_{16}C_2V^{2+}$, respectively ([Q] = 5×10^{-4} M, [NaLS] = 0.1 M), both at room temperature and at 77 K. Steady-state quenching measurements were also carried out for these systems at room temperature (for [Q] $\leq 2.5 \times 10^{-3}$ M). At room temperature, the time-dependent decay of the fluorescence was quite similar for the three systems. In actual fact, the Perrin plot for the steady-state quenching measurements showed good linearity for all of these three systems in the quencher concentration range used, the slopes being identical for all systems. In addition to the "dynamic" or "quasistatic"[24] quenching within the micelle, which appears as an initial fast decay, an appreciable reduction in fluorescence intensity immediately after laser excitation was observed for all systems. The intensity of the pyrene absorption spectrum around 337 nm also changes in the presence of these quenchers and an isosbestic point at 330 nm was observed. These data indicate an interaction of ground-state pyrene with the quenchers.[25] A ground-state complexation of pyrene and MV^{2+} in NaLS micelle by charge-transfer interaction has been reported.[26] A similar absorption change as that in a NaLS micellar solution was also observed for pyrene in a NaLS–EGW solution in the pressure of MV^{2+}, but the change in absorption is smaller and indicates a decreased association constant for the charge-transfer complexation[27] ($K_{asso} = 120\ M^{-1}$). This is probably due to the differing natures of the two micelles. The changes in the pyrene spectrum in the presence of CP^+, or $C_{16}C_2V^{2+}$, were smaller than those observed with MV^{2+}. The possible geometric arrangements of CP^+ and $C_{16}C_2V^{2+}$ with respect to pyrene are hindered compared to those of MV^{2+}; this is due to the interaction of the long hydrocarbon tails with the micelle. This may make it possible for MV^{2+} to occupy sites close to pyrene in the micelle. Lesser mobility is also expected for molecules which have a long hydrocarbon chain, especially in a "tight" micellar structure in an EGW solution. These data may explain the extent of ground-state complexation in the micelle. The above mentioned quenching result at room temperature can be understood by assuming that both static quenching through ground-state complexation and dynamic quenching through diffusional motion of solutes inside the micelle are taking place in these systems at room temperature. The similarity of steady-state quenching experiments for the three systems may show that the Poisson distribution of quenchers on micelles is not affected by the small amount of ground-state interaction of quenchers with probes.

The quenching behavior of these three species showed quite different features at 77 K, as shown in Figure 8. In the CP^+ system, only a single exponential decay whose lifetime is that of unquenched pyrene was observed. The fluorescence intensity at $t = 0$ was reduced at higher quencher concentrations, and inefficient quenching was observed at 77 K compared with that at room temperature. On the other hand, in the MV^{2+} system, effective quenching was observed at 77 K, i.e., an initial extremely fast decay was accompanied by a slow decay which was identical with an unquenched lifetime. In addition, a pronounced intensity reduction was also observed. For CP^+, it is absolutely necessary to have close contact with pyrene, through diffusional motion or complexation, in order to react with the excited state. Therefore the dynamic part of the quenching observed at room temperature is not observed in the rigid state at 77 K. Only those pyrene molecules that have an interaction with CP^+ in their ground state were subjected to quenching. In the MV^{2+}–pyrene system, however, the dynamic part of the quenching which took place at

(23) Menger, F. *Acc. Chem. Res.* **1979**, *12*, 111.

(24) Rogers, M. A. J.; Da Silva E Wheeler, M. F. *Chem. Phys. Lett.* **1978**, *53*, 165.

(25) It should be noticed that the absorption change in the presence of 5×10^{-4} M of these quenchers was negligible.

(26) Martens, F. M.; Verhoeven, J. W. *J. Phys. Chem.* **1981**, *85*, 1773.

(27) The association constant, K_{asso}, was obtained from the absorption change at 337 nm by utilizing the Benesi–Hildebrand method (Benesi, H. A.; Hildebrand, J. H. *J. Am. Chem. Soc.* **1949**, *71*, 2703) in this system. This method gave exactly the same value of $K_{asso} = 700\ M^{-1}$ that was recently estimated by using a charge-transfer band of the complex (ref 26), in 0.1 M NaLS solution.

room temperature appeared to become faster at low temperatures. This apparent fast quenching may be ascribed to the MV^{2+} frozen out at the originally solubilized sites close to pyrene in the micelle. However, at room temperature, increased mobility of the solutes may tend to separate them from each other within the lifetime of pyrene in the excited state. This gives rise to a slower quenching reaction at room temperature. The pronounced immediate intensity reduction at a low temperature may be explained by the increase in the association constant with decreasing temperature. In the $C_{16}C_2V^{2+}$ quenching system, the similarity of the time-dependent quenching at room temperature and at 77 K may be explainable by the assumption that reaction is possible for $C_{16}C_2V^{2+}$ without attaining close contact with excited pyrene. Diffusional motion at room temperature may serve only to average the reactants separation. Both CP^+ and MV^{2+} (or $C_{16}C_2V^{2+}$) are known to be good electron acceptors, and the viologen ion has a stronger electron affinity than the pyridinium ion. Accordingly, the above results strongly suggest the occurance of an electron-tunneling process, i.e., long-range electron transfer in the $C_{16}C_2V^{2+}$ system, although electron transfer is basically the mechanism also for CP^+ quenching. The strong dependence of the electron-transfer rate from the excited pyrene to viologen ion on the separation of quenchee–quencher pair supports this hypothesis.

Other quenchers for pyrene investigated in this study were Cu^{2+}, Eu^{3+}, Ag^+, Tl^+, *N,N'*-dimethylaniline (DMA), nitrobenzene (NB), and CCl_4. With metal ions, the effect of quencher on the time-dependent pyrene fluorescence decay is not appreciable at concentrations of less than several millimolar. This may be partly due to the decreased permeability of the micelle in an EGW solution compared to that of a normal NaLS micelle. The data emphasize the necessity of diffusional motion of metal ions for the quenching of singlet pyrene in micellar systems. However, at more than 10 mM, Cu^{2+} exhibited $C_{16}C_2V^{2+}$-type quenching, and both Ag^+ and Tl^+ exhibited MV^{2+}-type quenching. Pyrene phosphorescence was detected in the latter system,[28] and ground-state complexation was also detected in absorption-spectra studies. The quenching by DMA was classified into the CP^+ type although that by NB and by CCl_4 were of the $C_{16}C_2V^{2+}$ type. These quenchers are supposed to reside inside the micelle. The decreased quenching ability of DMA at 77 K may imply an importance of orientational factors for electron transfer in this system as well as the necessity of motion, since the separation of pyrene and DMA is expected to be small in these studies.

In conclusion, electron tunneling, i.e., long-range electron transfer, does not seem to be a predominant mechanism as far as common luminescence-quenching reactions in a micellar system at room temperature are concerned. Inhibition of motion by freezing in order to observe long-range phenomena is critical. The short lifetime of excited species also seems to contribute to the difficulty of instituting efficient tunneling processes. However, it is likely that more efficient tunneling becomes operative in certain triplet quenching reactions because of the longer lifetime of these excited states. The frozen micellar systems demonstrated here offer some advantages for studies to gain a better understanding of reactions on micelle, and also for long-range interactions.

Acknowledgment. The authors would like to thank the National Science Foundation for support of this work via Grant No. CHE 82-01226. Our thanks are also due to Mr. James Wheeler for writing the computer programs used to fit the experimental data. We are grateful to the reviewers for valuable comments.

Registry No. NaLS, 151-21-3; $Ru(bpy)_3^{2+}$, 74391-32-5; Cu^{2+}, 15158-11-9; Cr^{3+}, 16065-83-1; Fe^{3+}, 20074-52-6; $C_{16}C_2V^{2+}$, 78769-77-4; ethylene glycol, 107-21-1; pyrene, 129-00-0.

(28) The reaction of singlet pyrene with Ag^+ or Tl^+ is known to result in the intersystem crossing of pyrene. See, for example: Geacintov, N. E.; Prusik, T.; Khosrofian, M. *J. Am. Chem. Soc.* **1976**, *98*, 6444. Nosaka, Y.; Kira, A.; Imamura, M. *J. Phys. Chem.* **1981**, *85*, 1353.

Spin Inversion in the 1,4-Diradical Derived from 2,4,6-Triisopropylbenzophenone: Importance of Lone-Pair Orbital Rotation

Yoshikatsu Ito* and Teruo Matsuura

Contribution from the Department of Synthetic Chemistry, Faculty of Engineering, Kyoto University, Kyoto 606, Japan. *Received June 28, 1982*

Abstract: 4,6-Diisopropyl-2,2-dimethyl-1-phenyl-1,2-dihydrobenzocyclobuten-1-ol (**2**) was submitted to direct (254 nm) and sensitized photolysis and thermolysis in the absence or presence of oxygen. Direct photolysis (313 nm) of 2,4,6-triisopropylbenzophenone (**1**) was also performed in the absence or presence of oxygen. Interconversion between **1** and **2** and production of 1,3-diisopropyl-10,10-dimethylanthrone (**3**) and 1,4-dihydro-1-hydroxy-6,8-diisopropyl-4,4-dimethyl-1-phenyl-2,3-benzodioxin (**4**) happened in various quantum yields depending upon the reaction conditions. For example, the quantum yield of the transformation **2** → **1** was greatly different between direct ($\Phi = 0.2$) and triplet-sensitized ($\Phi = 0.7$, a limitting value) photolysis of **2**. It is deduced from analysis of measured product distributions (Φ(**1**) vs. Φ(**2**)) that quantum efficiencies for partitioning of a diradical intermediate DR are

$$\mathbf{1} \xleftarrow{0.22} {}^3\mathrm{A} \xrightarrow{0.78} \mathbf{2}, \quad \mathbf{1} \xleftarrow{0.2} {}^1\mathrm{B} \xrightarrow{0.8} \mathbf{2}, \text{ and } \mathbf{1} \xleftarrow{0.7} {}^3\mathrm{B} \xrightarrow{0.3} \mathbf{2}$$

where A (two face-to-edge odd orbitals) and B (two face-to-face odd orbitals) are different conformations of the same diradical species DR. This result led us to conclude that rotation of the lone-pair orbital in the diradical DR may create an effective vibrational overlap (Franck–Condon factor), leading to an efficient intersystem crossing of the diradical. It is also concluded that DR, which is generated from the direct photolysis of **1**, is spin protected and its lifetime is determined by the rate of intersystem crossing. The oxygen-trapping experiment indicated an unusually slow rate constant for reaction between DR and oxygen ($k_0' = 3.0 \times 10^7\ M^{-1}\ s^{-1}$).

Diradical chemistry is an active area of research both theoretically and experimentally. The most well-studied diradical species that are frequently encountered in organic reactions as unstable intermediates include type II diradicals,[2] Paterno–Büchi

0002-7863/83/1505-5237$01.50/0